



BUILDING A TALENT TRUST

**Department of Civil and
Environmental Engineering**

Faculty of Engineering

University of Waterloo
200 University Avenue West
Waterloo, Ontario, Canada

N2L 3G1

519-888-4494
Fax 519-888-4349
soudki@uwaterloo.ca

Flexural Behaviour of OctaformTM Concrete Forming System

Final Report

Prepared for

David Richardson, President
Octaform System Inc.
520-885 Dunsmuir St.
Vancouver, BC V6C 1N5

Prepared by

Khaled A. Soudki, PhD, PEng.
Professor and Canada Research Chair
and
Ahmad A. Rteil, PhD
Research Assistant

July 13, 2007

Abstract

Octaform™ system is a stay-in-place concrete forming system that consists of interconnected PVC elements. These elements are assembled (each element slides into the adjacent element) on the construction site into a hollow wall shell structure, which is then filled with concrete to complete the wall.

This report presents the observed and measured flexural behavior of twenty-four specimens fabricated using the Octaform™ system. All specimens were 305 mm wide and 2.5 m long. The variables studied were the depth of the specimen (150 mm or 200 mm), the steel reinforcement (none or two 10M bars), and the connector configuration. Two types of connectors were used: middle connectors and inclined (45°) connectors. The specimens were tested in horizontal position (to simulate flexural behaviour) in four point bending.

Results showed that the ultimate load for specimens encased with Octaform™ increased between 18% and 36% depending on the depth of the specimen and whether it was reinforced with steel bars or not. Octaform™ system also increased the cracking load, yield load and deflection for specimens with steel reinforcement on average by 36%, 78% and 40%, respectively. For specimens without steel reinforcement, the maximum load increased on average by 15% when both types of connectors were used as opposed to one type.

Table of Contents

Abstract	ii
Table of Contents	iii
List of Figures	iv
List of Tables.....	v
Chapter 1 Introduction.....	1
1.1 Octaform™ System	1
1.2 Shapes and Forms.....	1
1.3 Material Properties	2
1.4 Objectives of the Study	3
Chapter 2 Experimental Program	4
2.1 Test Program	4
2.2 Specimen Design.....	4
2.3 Specimen Fabrication	7
2.4 Material Properties	9
2.5 Test Setup and Instrumentation	10
Chapter 3 Experimental Results and Discussion.....	12
3.1 Behaviour of the Control Specimens (D6C and D8C)	12
3.2 Behaviour of the Octaform-Encased un-Reinforced Specimens	15
3.3 Behaviour of Octaform-Encased Reinforced Specimens	19
3.4 Effect of Octaform System.....	24
3.5 Effect of Steel Reinforcement	25
3.6 Effect of Connectors.....	26
Chapter 4 Conclusions.....	27
Appendix A Load-Deflection Behaviour	29
Acknowledgements	35
References	35

List of Figures

Figure 1.1 An assembled Octaform wall section	2
Figure 2.1 Cross section of a wall specimen with inclined connectors (Specimen D6I).....	6
Figure 2.2 Cross section of a wall specimen with middle connectors (Specimen D8M).....	6
Figure 2.3 Cross section of a wall specimen with middle and inclined connectors reinforced with steel bars (Specimen D8RIM)	7
Figure 2.4 Top view of the specimens before casting.....	8
Figure 2.5 Bracing system for the specimens	8
Figure 2.6 Placing concrete in the specimens	9
Figure 2.7 Concrete vibration	9
Figure 2.8 Strain gauge installed on the midspan section	10
Figure 2.9 Test setup.....	11
Figure 3.1 Typical crack distribution in the constant moment region	14
Figure 3.2 Concrete crushing in compression, a typical failure for control specimens	14
Figure 3.3 Typical load-deflection behaviour for control specimen.....	15
Figure 3.4 Typical crack distribution for encased un-reinforced specimens	16
Figure 3.5 Typical rupture of the Octaform panels.....	16
Figure 3.6 Load-deflection behaviour for Octaform-encased un-reinforced specimens.....	18
Figure 3.7 Typical Octaform tension strain behaviour for encased un-reinforced specimens (specimen D6MI-2)	19
Figure 3.8 Typical concrete crack distribution for Octaform-encased reinforced specimens.....	20
Figure 3.9 Typical compression failure for Octaform-encased reinforced specimens.....	20
Figure 3.10 A crack in a tension panel in the Octaform-encased reinforced specimens	21
Figure 3.11 Load-deflection behaviour of the control and reinforced Octaform-encased specimens .	22
Figure 3.12 Typical permanent deflection for reinforced Octaform-encased specimens (specimen is shown upside down)	23
Figure 3.13 Typical tension strain variation for an Octaform tension panel (specimen D6RI-1).....	23
Figure 3.14 Effect of steel reinforcement	25

List of Tables

Table 1.1: Mechanical properties of the Octaform system (Octaform general guide, 2004)	3
Table 2.1 Test matrix.....	5
Table 3.1: Test results	13

Chapter 1

Introduction

1.1 Octaform™ System

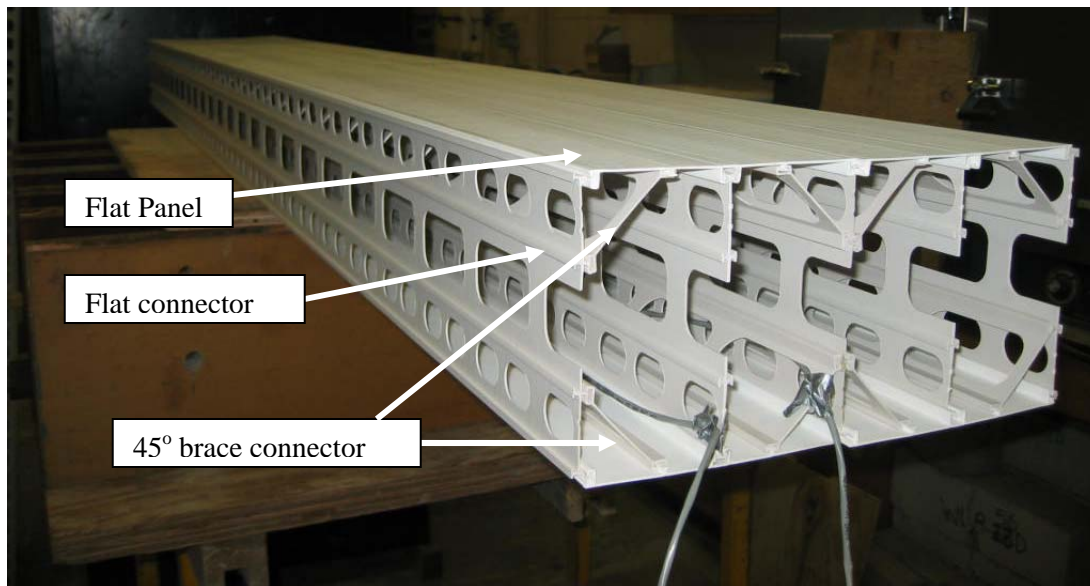
The Octaform™ wall system is a stay-in-place concrete forming system. It consists of interconnected PVC elements that are assembled (each element slides into the adjacent element) on the construction site into a hollow wall shell structure, which is then filled with concrete to complete the wall. It should be noted that the hollow wall structure should be braced and scaffolding erected as per the requirements of Octaform before pouring concrete (Octaform, 2004). The PVC elements are made of high quality polymers. A series of openings in the interconnecting elements allow for easy installation of reinforcing steel and the lateral flow of concrete (Octaform, 2004).

The wall system is supplied in varying depths (4 to 12 inches, in two-inch increments). Octaform™ wall elements have the flexibility to be assembled to create either straight or round walls. The elements totally confine the reinforced concrete wall structure, which allows for an increase in the strength and durability of the structure (Octaform, 2004).

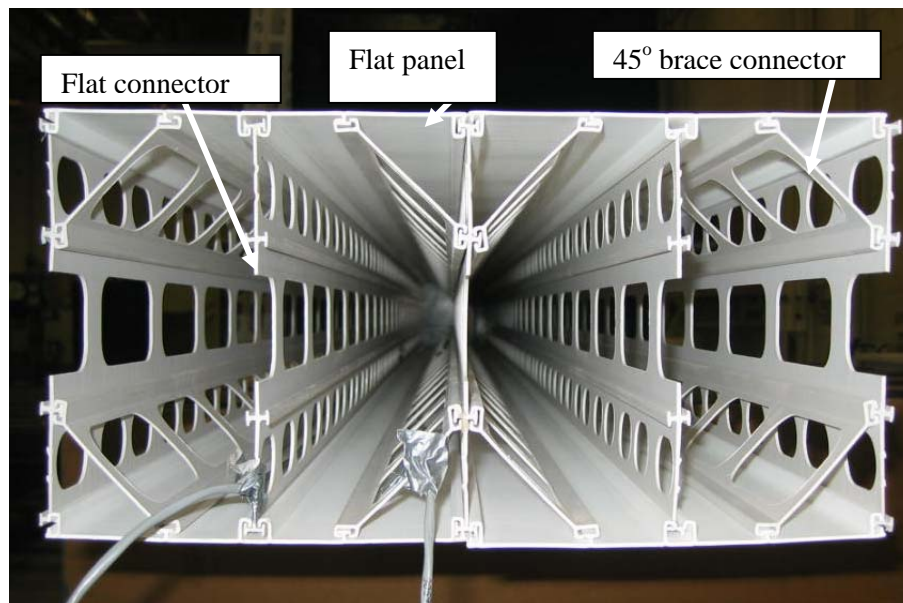
The Octaform wall system can be used as foundation walls, retaining walls, water and waste treatment tanks, noise abatement walls, and swimming pools. It is used in agricultural, industrial and residential buildings.

1.2 Shapes and Forms

The elements of the Octaform system are composed of panels (flat, corrugated or curved) and connectors. The connectors are punched with open holes. The panels are used to erect the two faces of the wall, which are connected by the hollow connectors (Figure 1.1).



a) Side view



b) Cross section view

Figure 1.1 An assembled Octaform wall section

1.3 Material Properties

The elements of the Octaform system are made from rigid polyvinyl chloride (PVC). The mechanical properties of the flat panels are given in Table 1.1. The PVC by itself does not burn and is very

difficult to ignite (temperature required to ignite PVC approximately 427°C (800°F)). A fully constructed Octaform wall has at least a two-hour fire rating (Octaform, 2004).

Table 1.1: Mechanical properties of the Octaform system (Octaform general guide, 2004)

Tensile yield strength, MPa (ksi)	45.8 (6.64)
Tensile modulus of elasticity, MPa (ksi)	2772 (402)
Flexural strength, MPa (ksi)	81 (11.7)
Flexural modulus of elasticity, MPa (ksi)	2661 (386)
Coefficient of thermal expansion, 10 ⁻⁵ /°C (10 ⁻⁵ /°F)	6.7 (3.7)

1.4 Objectives of the Study

The main objective of this study was to investigate the flexural behaviour of concrete walls encased with Octaform system. The effects of different connector configurations, wall thickness and steel reinforcement on the flexural behaviour of an Octaform™ encased wall were also studied.

Chapter 2

Experimental Program

2.1 Test Program

Twenty-four (24) specimens were cast and tested in the Structures Laboratory at the University of Waterloo. The specimens were divided into twelve groups. Each group had two duplicate specimens. Table 2.1 identifies the test matrix. Four specimens were cast and tested without the Octaform™ system to act as control. The other twenty specimens were cast in the concrete forming system. The variables studied in these specimens were the specimen depth (150 mm or 200 mm (6 in or 8 in)), the amount of steel reinforcement (none or two 10M bars), and the connector configuration. Two types of connectors were used: middle connectors and inclined (45°) connectors.

2.2 Specimen Design

The specimen used in this study had a rectangular cross section. The width of all the specimens was 305 mm (12 in) made by using two 152 mm (6 in) wide panels. The length was 2.5 m (96 in). The depth of the specimen was 150 mm or 200 mm (6 in or 8 in) varied as seen in Table 2.1. All the specimens encased with Octaform™ system were made by assembling four panels (each two forming one surface of the wall), a flat connector between the panels (dividing the wall specimen into two cells) and another two flat connectors forming the sides of the wall specimen. For the specimens with middle connector configuration (letter M in the specimen notation), an additional two flat connectors were installed in the middle of each cell of the specimen (Figure 2.1). The specimens with inclined connector configuration (letter I in the specimen notation) were made by installing eight (8) 45° connectors in the eight corners of the specimen (Figure 2.2). The specimens reinforced with steel reinforcement (letter R in the specimen notation) had two 10M steel bars fixed at the tension side of the specimen, 25 mm (1 in) away from the panel surface (Figure 2.3).

Table 2.1 Test matrix

Group*	Specimen depth (mm)	Steel reinforcement (10M bars)	Cast in Octaform system	Connector configuration (inclined/middle)
D6C-1 D6C-2	150	2	No	None
D6RI-1 D6RI-2			Yes	Inclined
D6RIM-1 D6RIM-2				Inclined and Middle
D6I-1 D6I-2		Inclined		
D6M-1 D6M-2		None		Middle
D6MI-1 D6MI-2			Inclined and Middle	
D8C-1 D8C-2		200	2	No
D8RI-1 D8RI-2	Yes			Inclined
D8RIM-1 D8RIM-2				Inclined and Middle
D8I-1 D8I-2			Inclined	
D8M-1 D8M-2			None	Middle
D8MI-1 D8MI-2			Inclined and Middle	

* DXY-A: X = 6 or 8 for the 150 or 200 mm depth respectively.

Y = C for control, R for steel reinforcement, I for inclined (45°) connector, and M for middle connector

A = 1 or 2 to differentiate the two specimens

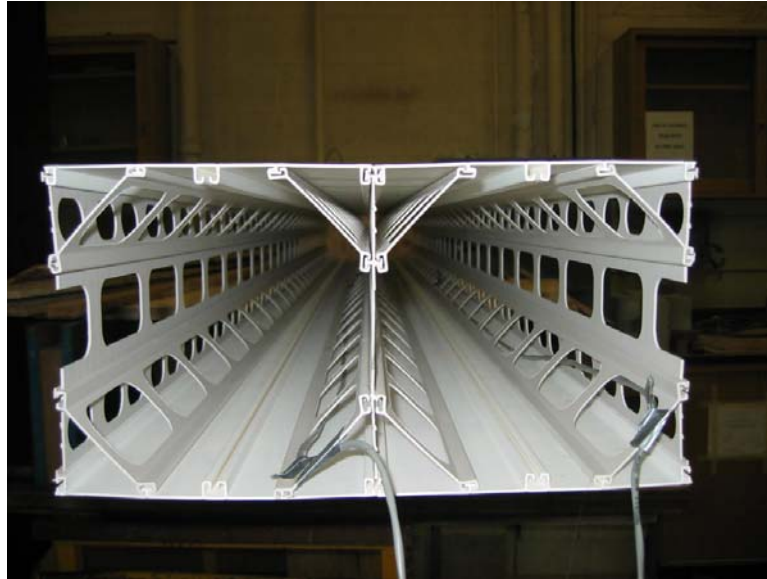


Figure 2.1 Cross section of a wall specimen with inclined connectors (Specimen D6I)

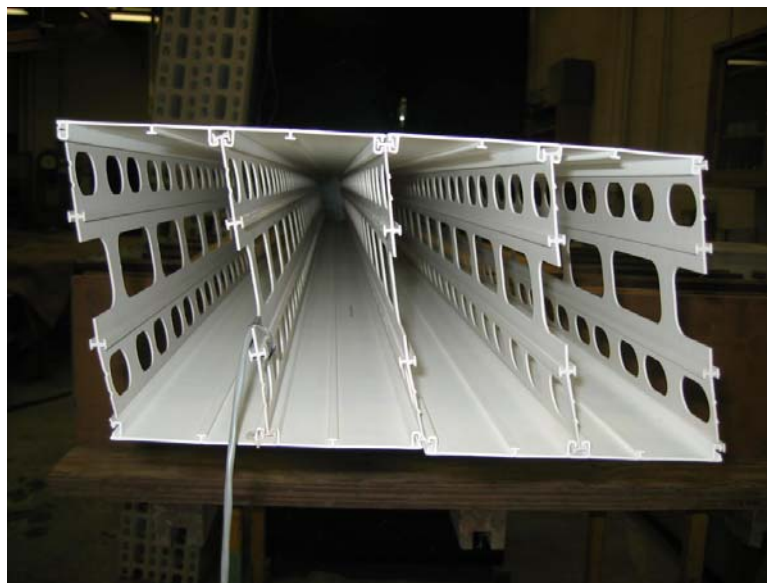


Figure 2.2 Cross section of a wall specimen with middle connectors (Specimen D8M)

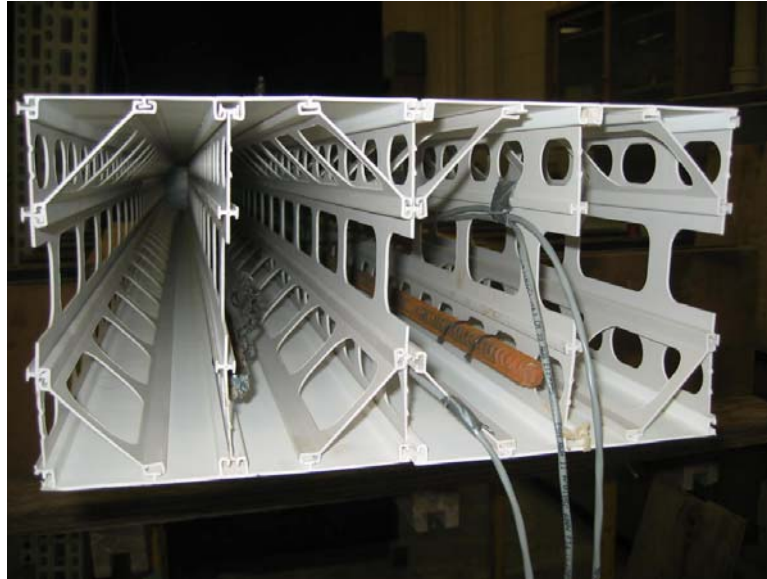


Figure 2.3 Cross section of a wall specimen with middle and inclined connectors reinforced with steel bars (Specimen D8RIM)

2.3 Specimen Fabrication

Each specimen was assembled using the panels, connectors and steel reinforcement as explained in the previous section. The specimens were cast vertically typical to the construction practice. The specimens were placed in rows. Each row had four or five specimens placed surface to surface. The rows were separated by reusable plywood sheets (38 mm thick) that sealed the sides of the wall specimens (Figure 2.4). The specimens were then braced using 2x4 studs (Figure 2.5).

The concrete was supplied by a local ready mix plant with a slump of 180 mm. The concrete was poured using a bucket until the walls were completely filled (Figure 2.6), then the specimens were vibrated using a hand vibrator that was long enough to reach the bottom of the specimen (Figure 2.7). Several concrete cylinders (100 mm x 200 mm) were cast with the walls for later use in measuring the compression strength. A few hours after the casting, the forms were covered by wet burlap for curing for about 7 days.

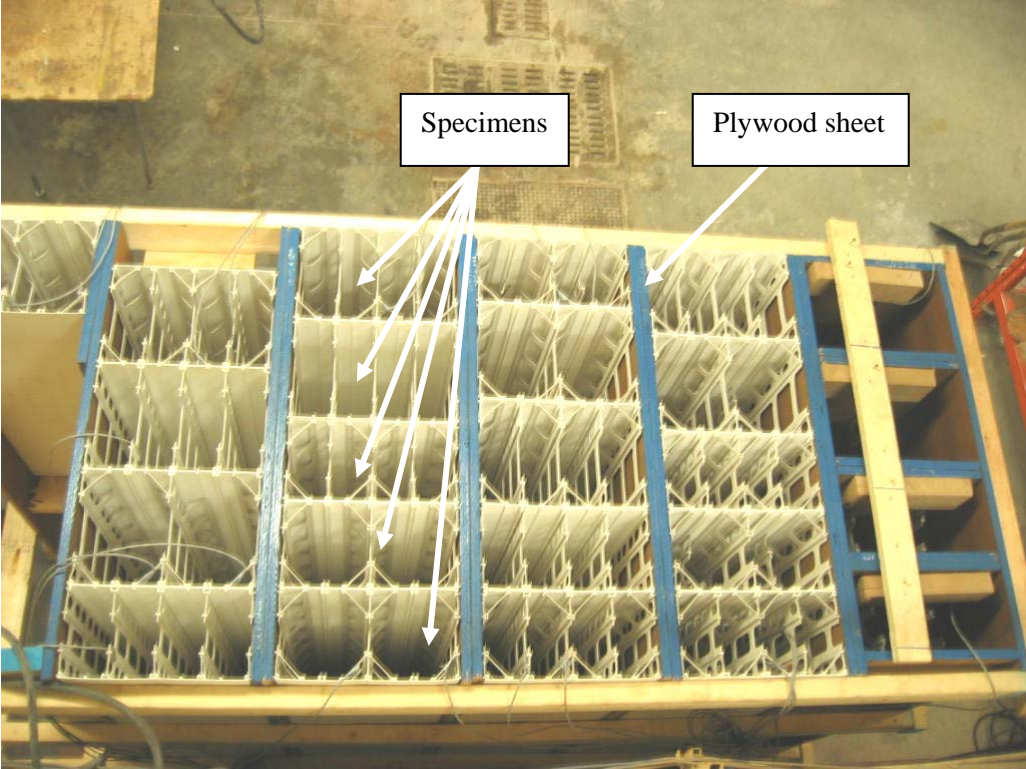


Figure 2.4 Top view of the specimens before casting



Figure 2.5 Bracing system for the specimens



Figure 2.6 Placing concrete in the specimens



Figure 2.7 Concrete vibration

2.4 Material Properties

The concrete had a measured 28 days compressive strength of 25 MPa, representing a typical concrete strength used in practice. The measured compressive strength at the time of testing (63 days)

was around 38 MPa. The steel reinforcement used in this study were 10M bars (diameter 11.3 mm) and had a nominal yield strength of 400 MPa.

2.5 Test Setup and Instrumentation

All the specimens were instrumented with one electrical strain gauge at each surface, one surface was in tension and the other was in compression. The strain gauges were installed at the midspan section (Figure 2.8) and had a gauge length of 5 mm and a resistance of 120 Ω .

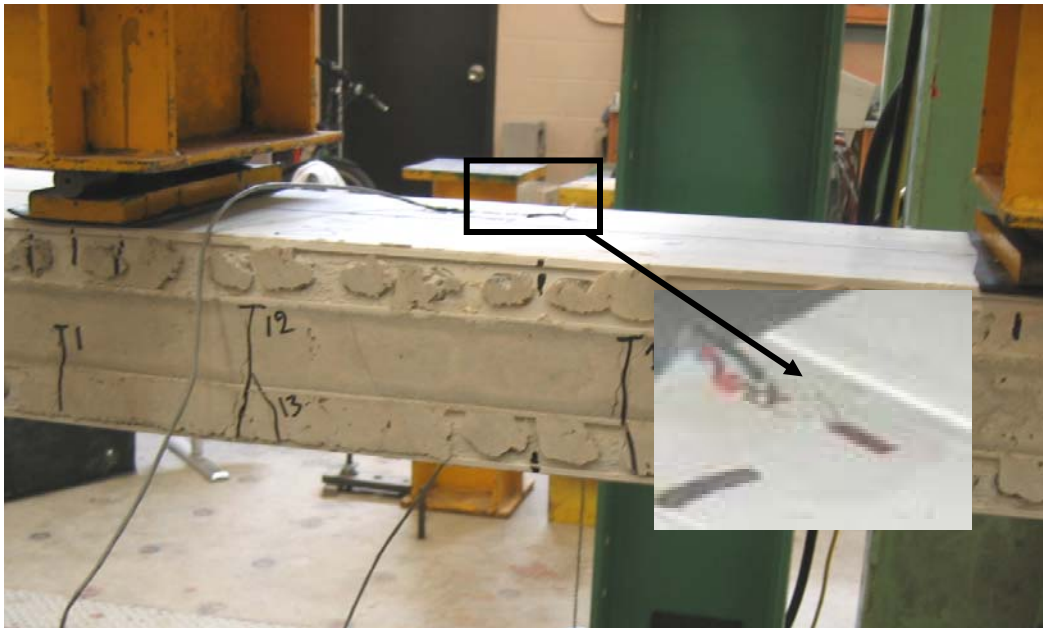


Figure 2.8 Strain gauge installed on the midspan section

The specimens were tested in a horizontal position in four point bending (Figure 2.9) with a total span of 2100 mm and a constant moment region of 700 mm. The load was applied using a servo-hydraulic actuator, with a capacity of 220 kN (50 kips), controlled by a Material Testing System (MTS) 407 controller. The tests were performed in stroke control at a rate of 1.5 to 2.0 mm/min. One Linear Variable Differential Transformer (LVDT) with a 100 mm stroke range was used (Figure 2.9) to monitor the beam's deflection at mid-span. The specimen was loaded until it failed. The failure of

the specimen was defined as a 25% drop in the load compared to its maximum attained value. The duration of each test was around 2 hours.

The readings from the strain gauges, load cell and LVDT were collected and stored by a computer based National Instrument data acquisition system.

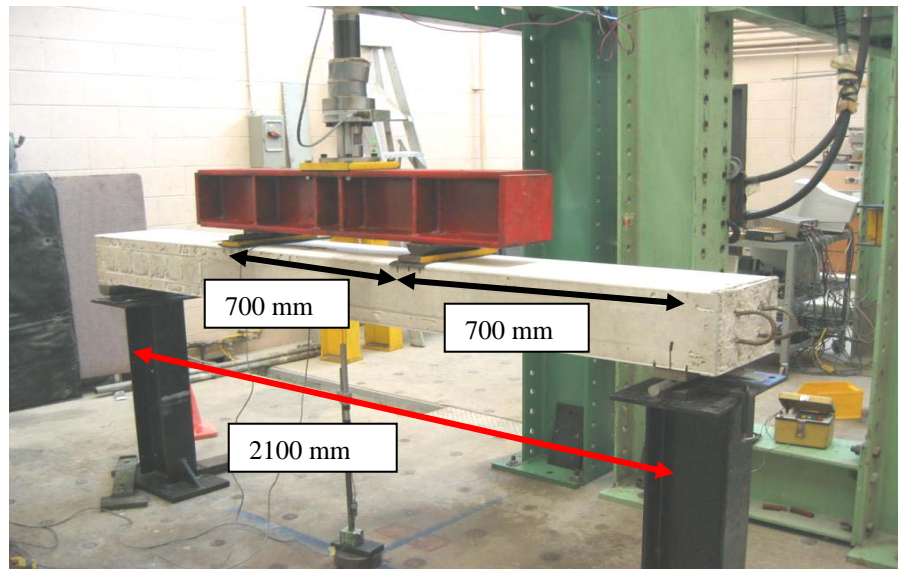


Figure 2.9 Test setup

Chapter 3

Experimental Results and Discussion

This chapter presents the experimental results of the control specimens and those encased with Octaform system. The discussion will focus on the general behaviour, the failure mode, and the load-deflection response. The discussion is based on the observations and test data collected during the tests. In general, the behaviour (cracking load, stiffness, yielding load, crack distribution, etc) of the two duplicate specimens in each group was very similar (see Appendix A). Accordingly, the discussion in this chapter is based on the average behaviour of the two duplicate specimens tested in each group. Table 3.1 presents the values of the load and the corresponding deflection for each beam at the onset of cracking, steel yielding, and Octaform yielding. It also gives the attained maximum load and the maximum deflection.

3.1 Behaviour of the Control Specimens (D6C and D8C)

3.1.1 General Behaviour and Mode of Failure

For the control reinforced concrete specimens (D6C and D8C) the first flexural crack appeared in the constant moment region (between the two loading points). As the load increased, additional flexural cracks opened in the constant moment region and in the shear span and started to propagate along the depth of the specimen (Figure 3.1). Once the steel reinforcement yielded, the crack growth stabilized, but their width continued to increase. Just before failure, the concrete in the compression surface (in the constant moment region) started to crush. The mode of failure for the control beams was concrete crushing in compression after yielding of the steel reinforcement (Figure 3.2).

Table 3.1: Test results

Group	Cracking		Steel yield		Octaform yield		Maximum	
	Load (kN)	Deflection (mm)	Load (kN)	Deflection (mm)	Load (kN)	Deflection (mm)	Load (kN)	Deflection (mm)
D6C-1	9.58	1.35	32.58	14.53	--	--	39.4	146
D6C-2	12.52	2.01	31.7	13.8	--	--	40.2	182
D6RI-1	17.8	2.14	40.7	13.50	52.5	49.5	54.3	156
D6RI-2	17.2	0.87	42	11.85	52.5	53	53.7	178
D6RIM-1	16	1.43	42.73	15.9	53.5	55.6	54.7	258
D6RIM-2	16	3.5	41.5	16.4	52.7	49	54.5	229
D6I-1	13.8	1.32	--	--	16.8	38.6	16.5	119
D6I-2	14.9	1.5	--	--	16.8	35.8	17	58.6
D6M-1	12.5	1.55	--	--	14.61	37	14.9	212
D6M-2	14.6	1.61	--	--	15.7	34	15.8	65.4
D6MI-1	11.71	1.47	--	--	18.4	48	18.5	211
D6MI-2	12.76	1.37	--	--	19.3	47.6	19.5	120
D8C-1	21.9	1.68	36.7	8.5	--	--	53.9	125
D8C-2	18.8	1.18	42.1	9.9	--	--	57.2	141
D8RI-1	25	1.95	59.6	11.97	78	53	79	175
D8RI-2	35	1.73	60	10.4	73	50	74	204
D8RIM-1	21	1.5	57	11.8	74	47	76	224
D8RIM-2	26	1.87	63	11.8	78	45	79	253
D8I-1	24.5	0.17	--	--	22	12	24.5	22
D8I-2	28	1.4	--	--	24	13	28	49
D8M-1	23.7	1.68	--	--	22	15	24	102
D8M-2	23.6	1.78	--	--	24	22	24.5	33
D8MI-1	21.02	2.24	--	--	26	25	27	101
D8MI-2	29.6	2.32	--	--	26	24	29.6	77

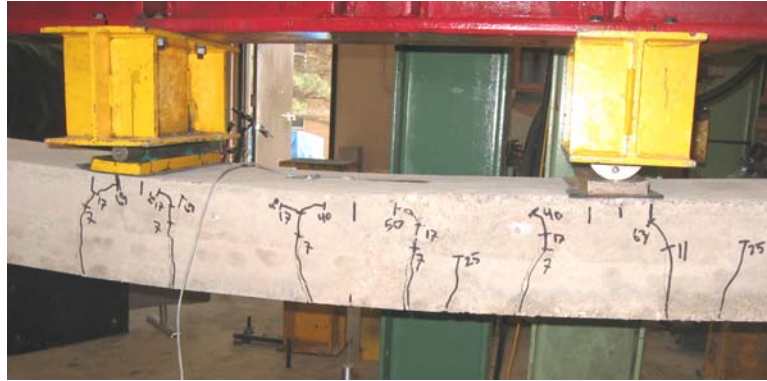


Figure 3.1 Typical crack distribution in the constant moment region



Figure 3.2 Concrete crushing in compression, a typical failure for control specimens

3.1.2 Flexural Behaviour

The cracking load was on average (two duplicate specimens) 12 kN and 20 kN for specimens D6C and D8C respectively (Figure 3.3). As the deflection increased, the load increased linearly up to the yield load (Figure 3.3). The average yield load (two duplicate specimens) was 32 kN and 39.5 kN for specimens D6C and D8C respectively. After yielding, the load increased linearly until failure.

However, the stiffness (the slope of the load-deflection curve) of the pre-yielding was much higher than that of the post-yielding (Figure 3.3). The maximum load attained by the control specimens was

on average 40 kN and 55.5 kN for specimens D6C and D8C respectively. The deflection at failure for the control specimens was 166 mm and 138 mm for specimens D6C and D8C respectively. The deflection ductility index (maximum deflection divided by yielding deflection) for the control specimens was 11 and 16 for specimens D6C and D8C respectively.

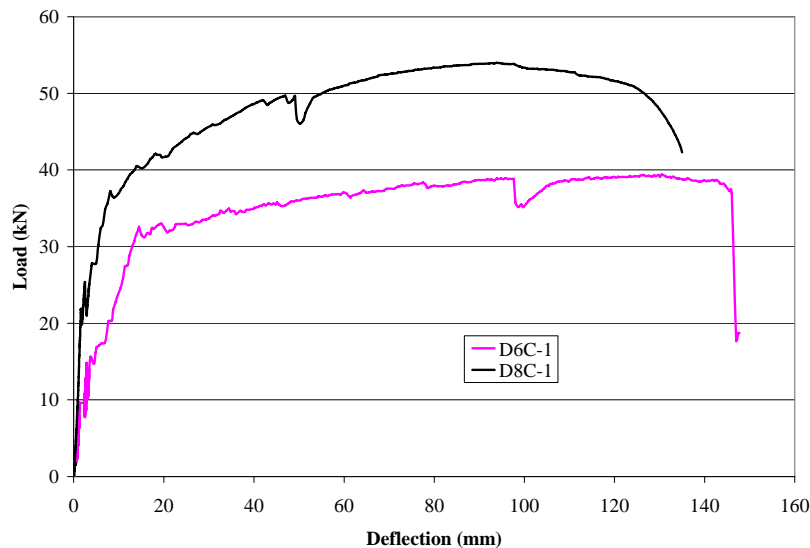


Figure 3.3 Typical load-deflection behaviour for control specimen

3.2 Behaviour of the Octaform-Encased un-Reinforced Specimens

The Octaform-encased un-reinforced specimens are the specimens that were encased with Octaform system, but had no steel reinforcement (Groups D6I, D6M, D6MI, D8I, D8M, and D8MI).

3.2.1 General Behaviour and Mode of Failure

In general, as the load increased, a flexural crack appeared in the constant moment region. This crack caused the load to drop suddenly. The load resumed increasing afterwards until a second flexural crack opened where the load dropped again and then increased. This behaviour was repeated in all the encased un-reinforced specimens each time a new concrete crack opened. However, since the specimens were not reinforced with internal steel bars, only one to three flexural cracks opened during testing (Figure 3.4). As the PVC yielded, the load stabilized and the width of the existing

cracks increased. This stage continued until one of the tension Octaform panels ruptured. Then the load decreased significantly and the specimen failed. The Octaform rupture was accompanied by a loud noise and it normally took place underneath one of the flexural concrete cracks (Figure 3.5).



Figure 3.4 Typical crack distribution for encased un-reinforced specimens



Figure 3.5 Typical rupture of the Octaform panels

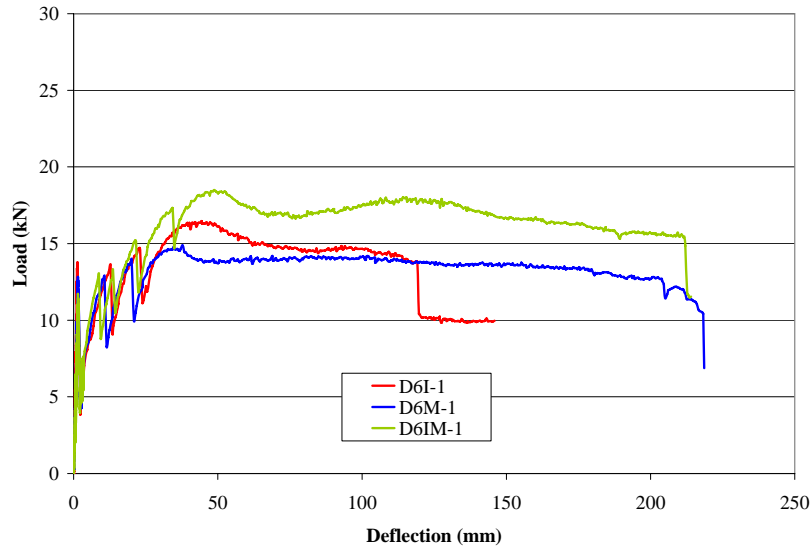
3.2.2 Flexural Behaviour

The load deflection behaviour of the encased un-reinforced specimens could be divided into three stages (Figure 3.6). In the first stage (pre-cracking), the load increased linearly with deflection. The cracking load was on average 12 kN for specimens with 150 mm (6 in) depth and 25 kN for specimens with 200 mm (8 in) depth similar to the control specimens. After the first concrete flexural crack took place, the second stage started. This stage was characterized by saw-teeth load-deflection behaviour (Figure 3.6). The saw-teeth behaviour was due to multiple flexural cracks that opened in concrete. After each concrete crack, the load dropped significantly, meanwhile, the tension forces in the concrete were transferred to the Octaform tension panels. The saw-teeth stage continued until the Octaform tension panels yielded. The yield load was around 16 kN and 24 kN for the 150 mm (6 in) and 200 mm (8 in) deep specimens respectively. In the third stage, the load either dropped gradually or was stable. This continued until one of the tension Octaform panels ruptured, then the load dropped significantly and the specimen failed. The maximum load attained by the un-reinforced Octaform encased specimens was on average 17 kN and 26 kN for specimens with 150 mm and 200 mm depth respectively.

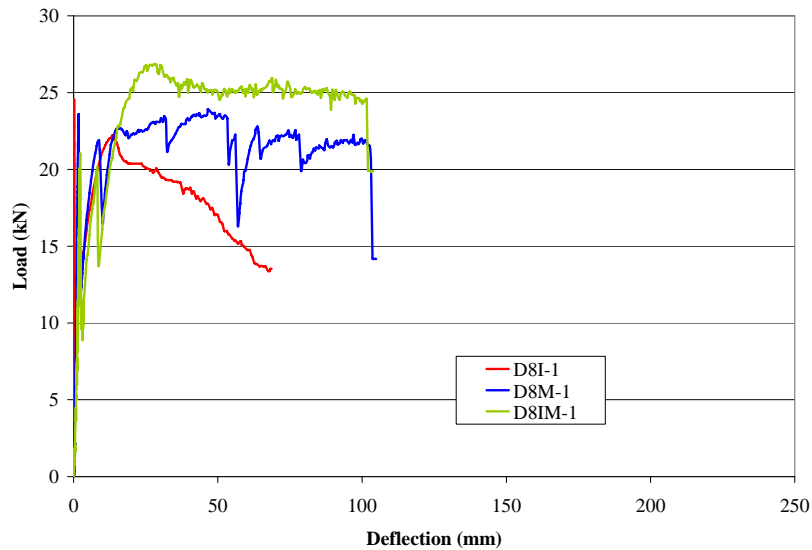
3.2.3 Octaform Tension Strain Behaviour

The strain of the Octaform tension panels was measured by an electrical strain gauge attached to one of the two tension panels at midspan (see section 2.5). In the pre-cracking stage, the Octaform panels carried virtually no load (see Figure 3.7). Once the concrete cracked, the tension forces were transferred from the concrete to the panels at the crack location. This increased the stress in the Octaform panels (see Figure 3.7). As the concrete had multiple cracks, the stress in the Octaform tension panels continued to increase until their yield. The yielding strain for the Octaform panels was on average 13,000 $\mu\epsilon$ (ranged from 8,200 $\mu\epsilon$ to 20,000 $\mu\epsilon$) for all the Octaform-encased un-reinforced

specimens, irrespective of the specimen depth. After yielding, the strain increase was small until failure (panel rupture).



a) Specimens with 150 mm depth



b) Specimens with 200 mm depth

Figure 3.6 Load-deflection behaviour for Octaform-encased un-reinforced specimens

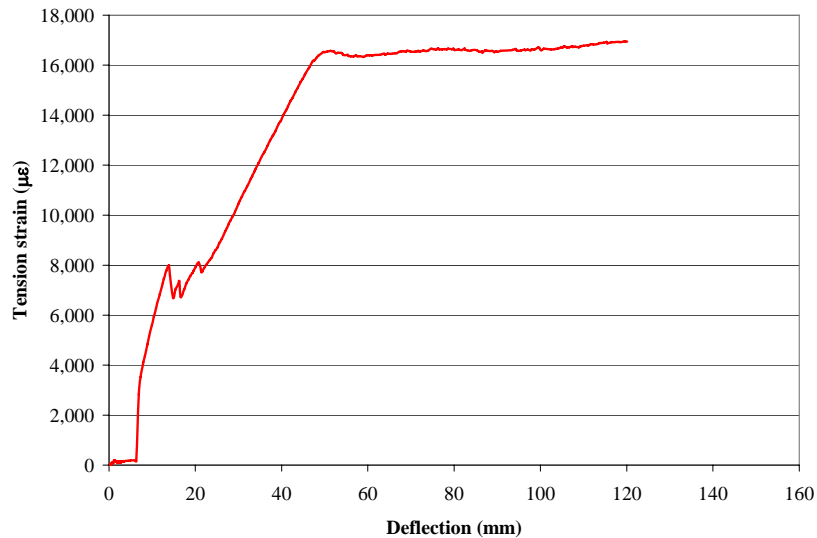


Figure 3.7 Typical Octaform tension strain behaviour for encased un-reinforced specimens (specimen D6MI-2)

3.3 Behaviour of Octaform-Encased Reinforced Specimens

The Octaform-encased reinforced specimens are the specimens that were encased with Octaform system, and reinforced with 2-M10 steel bars (Groups D6RI, D6RIM, D8RI, and D8RIM).

3.3.1 General Behaviour and Mode of Failure

The behaviour of the Octaform-encased reinforced specimens was similar to that of the control specimens (see section 3.1.1). The first concrete crack appeared in the constant moment region. As the load increased, several other cracks initiated and propagated along the depth of the specimen (Figure 3.8). Unlike the un-reinforced Octaform encased specimens, the concrete cracks in this group did not cause the load to drop, instead the load continued to increase until the Octaform yielded. After the yield load was reached, the width of the concrete cracks increased and some cracks propagated further. As the test continued, the compression Octaform panels started to pop-out (separation between Octaform panels and concrete) and the compression concrete to crush (Figure 3.9). The failure of the specimen occurred when the concrete crushed completely and the Octaform panel

buckled (Figure 3.9). It is important to note that the Octaform tension panels either ruptured, had a small crack, or did not crack at all (Figure 3.10).



Figure 3.8 Typical concrete crack distribution for Octaform-encased reinforced specimens



a) Octaform buckling



b) Concrete crushing

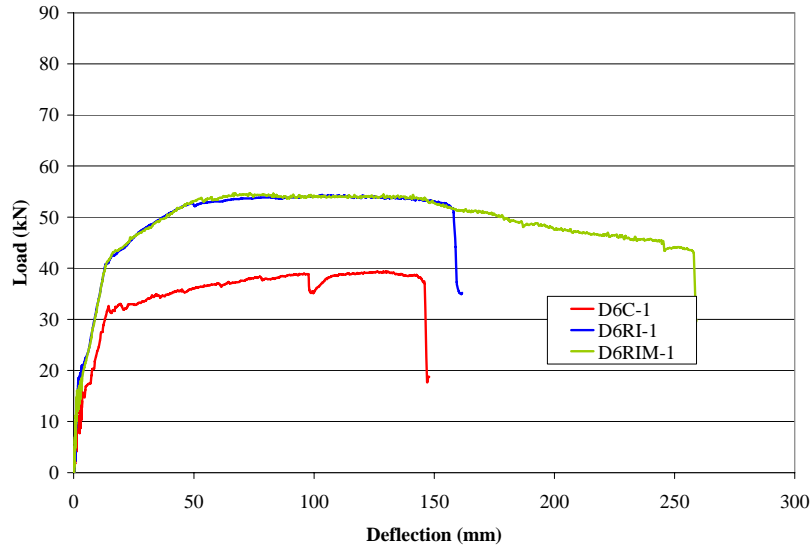
Figure 3.9 Typical compression failure for Octaform-encased reinforced specimens



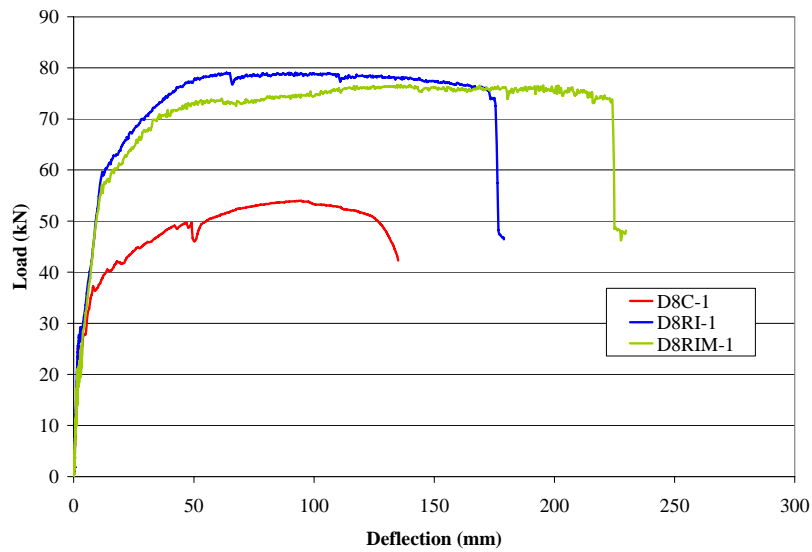
Figure 3.10 A crack in a tension panel in the Octaform-encased reinforced specimens

3.3.2 Flexural Behaviour

The load deflection curves for the Octaform-encased reinforced specimens are shown in Figure 3.11. In general, the load-deflection curve could be divided into four stages (Figure 3.11). In the first stage (pre-cracking stage), the load increased linearly with deflection. Once the first concrete crack appeared the stiffness of the specimen decreased, however, the load-deflection relationship continued to be linear (Figure 3.11). The cracking load was around 16.5 kN and 25 kN for the 150 mm and 200 mm wide specimens respectively. The third stage started when the steel reinforcement yielded. The steel reinforcement yielded at around 41 kN and 60 kN for the 150 mm and 200 mm wide specimens respectively. The yielding of the steel reinforcement decreased the stiffness further (Figure 3.11). In the fourth stage, the Octaform tension panels yielded and the load ceased to increase (Figure 3.11). This stage ended when the concrete crushed and the compression Octaform buckled signifying specimen failure. The maximum load attained by the specimens was on average 54 kN and 77 kN for the D6 and D8 specimens respectively. The deformation ductility index for all the specimens in this group was on average 4.0 (Figure 3.12).



a) Specimens with 150 mm depth



b) Specimens with 200 mm depth

Figure 3.11 Load-deflection behaviour of the control and reinforced Octaform-encased specimens



Figure 3.12 Typical permanent deflection for reinforced Octaform-encased specimens (specimen is shown upside down)

3.3.3 Octaform Tension Strain Behaviour

The strain in the Octaform tension panel in the pre-cracking stage was negligible (Figure 3.13). However, once the first concrete crack took place, the stress in the Octaform panels increased. The increase was exponential (Figure 3.13). The strain continued to increase gradually until the steel reinforcement yielded. Then the stress in the Octaform started to increase at a higher rate until the specimen failed (or the strain gauge failed) (Figure 3.13).

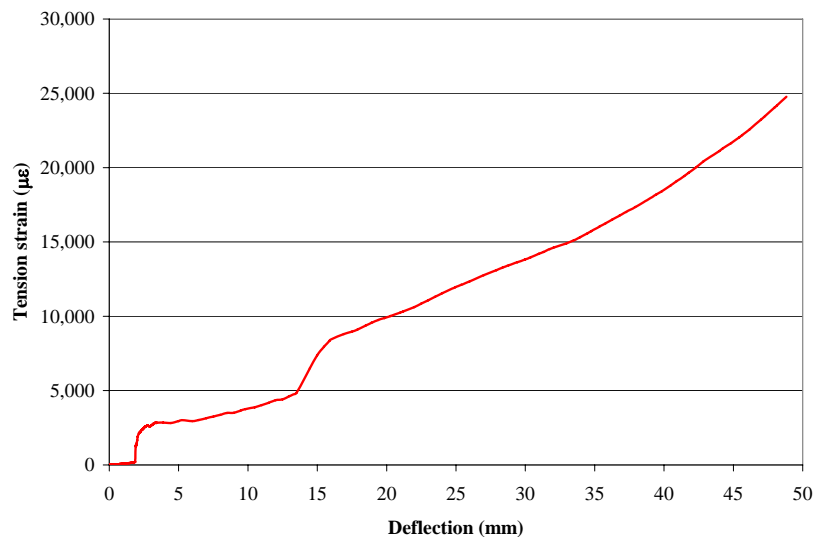


Figure 3.13 Typical tension strain variation for an Octaform tension panel (specimen D6RI-1)

3.4 Effect of Octaform System

The effect of Octaform system could be best understood by comparing the encased un-reinforced specimens to plain concrete fracture strength and by comparing the encased reinforced specimens to the control specimens.

The concrete fracture strength (f_r) is given as a function of the concrete compressive strength (f'_c) in CSA 23.3-04 as:

$$f_r = 0.6\sqrt{f'_c} \quad \text{Equation 3.1}$$

For a concrete of compressive strength of 38 MPa, the fracture strength is equal to 3.7 MPa. This means that a plain concrete specimen similar to the ones used in this study (without steel reinforcement and not encased in Octaform) would fail at a fracture load of 12.5 kN and 22 kN for 150 mm and 200 mm beam depth respectively. These values are very close to the experimental cracking loads (12 kN for specimens with 150 mm (6 in) depth and 25 kN for specimens with 200 mm (8 in) depth, see section 3.2.2) for Octaform-encased un-reinforced specimens. A plain concrete specimen (not encased with Octaform and without steel reinforcement) would fail at the onset of concrete cracking. However, the presence of the Octaform in the specimens tested in this study increased the load-carrying capacity of the specimen by 36% and 18% for D6 and D8 specimens respectively. The addition of Octaform also increased the deflection from an average of 1.5 mm (at the cracking load) to about 100 mm (maximum deflection attained just before failure).

For specimens reinforced with steel bars, the presence of Octaform increased the cracking load by about 36% compared to the control specimens. It also increased the yield load by 65% and 91% for D6 and D8 specimens respectively and the maximum load by about 36% for both D6 and D8 specimens (Figure 3.11). It is also noted that the maximum deflection capacity of the Octaform-encased specimens increased by 24% and 55% for D6 and D8 respectively compared to the control specimens.

3.5 Effect of Steel Reinforcement

The effect of steel reinforcement is determined by comparing groups D6I, D8I, D6IM and D8IM with groups D6RI, D8RI, D6RIM and D8RIM respectively.

The steel reinforcement had two main effects on the performance of the wall specimens. The number of cracks increased but their width decreased in specimens with steel reinforcement compared to their counterparts without steel reinforcement (Figure 3.4 and Figure 3.8). The presence of steel reinforcement eliminated the saw-teeth behaviour observed in the load-deflection curve of the unreinforced specimens, where the load dropped suddenly each time the concrete cracked. Instead, in the reinforced specimens the load increased continuously with the deflection up to yielding, followed by an increase in deflection with minor increase in load (Figure 3.14).

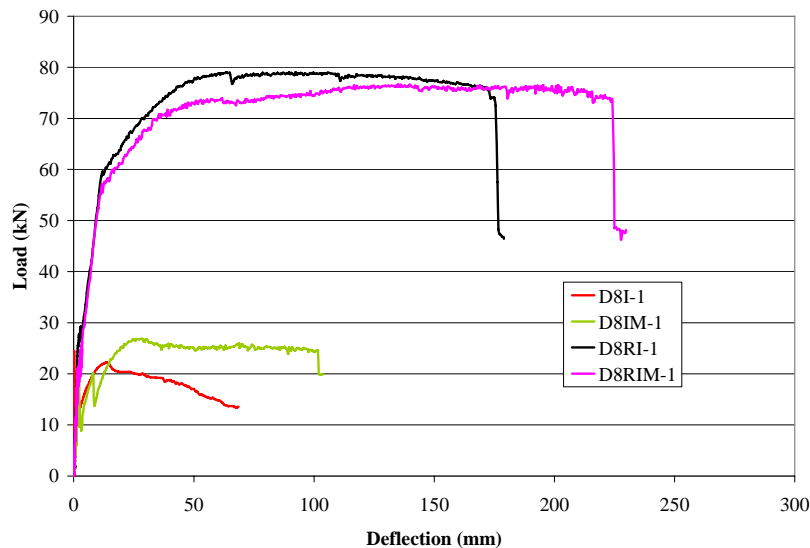


Figure 3.14 Effect of steel reinforcement

The second effect of the steel reinforcement was the increase in the load and deflection capacities. The maximum load increased by 181% and 205% for specimens IM and specimens I with steel reinforcement (RIM and RI) compared to those without steel reinforcement. This increase was independent of the depth of the specimens. The increase in the maximum deflection ranged from 50%

for specimen D6RIM (compared to specimen D6MI) to 4.3 times for specimen D8RI (compared to specimen D8I).

3.6 Effect of Connectors

In this study two different connectors were used, the 45° connector placed at the corner of the two compartments of the specimen (Figure 2.1) and the flat connector placed in the middle of each compartment (Figure 2.2). The effect of these connectors is evaluated by comparing specimen RI with specimen RIM (the effect of middle connector) and specimen IM with specimen I and specimen M (the effect of the middle and inclined connectors respectively).

Figure 3.11 show the load-deflection behaviour of specimens D6RI, D6RIM, D8RI and D8RIM. In general, there was virtually no difference in the behaviour of these specimens in terms of cracking load, stiffness, yield load and maximum load. This suggests that the presence of the middle connector did not alter the performance of the Octaform-encased specimens reinforced with steel bars.

On the other hand, the connectors had a pronounced effect in the Octaform-encased specimens with no steel reinforcement (Figure 3.6). The maximum load increased by about 10% in specimen IM compared to that of specimen I and by 19% compared to specimen M. In addition, the yield load of specimen IM increased by 12% compared to specimen I and by 18% compared to specimen M. The increase was independent of the depth of the specimens. However, there was no difference between specimen M and specimen I. This implies that the use of both connectors (specimen IM) not only enhanced the rigidity to the specimens before concrete casting, but also increased the yield and maximum load compared to using only one connector type (specimen I and specimen M).

Chapter 4

Conclusions

Based on the present study, the use of the Octaform forming system enhanced the behaviour (strength and ductility) of plain and steel reinforced concrete flexural members. Specifically, the following conclusions are drawn.

- The presence of the Octaform system in un-reinforced specimens (without steel reinforcement)
 - a. Increased the load-carrying capacity by 36% and 18% for specimens with 150 mm and 200 mm depth respectively compared to plain concrete specimens (without steel reinforcement and not encased with Octaform system).
 - b. Increased the deflection of the un-reinforced specimens from an average of 1.5 mm (at the cracking load) to about 100 mm (deflection attained just before failure).
- The presence of Octaform in specimens reinforced with steel bars:
 - a. Increased the cracking load by about 36% compared to the control specimens (reinforced with steel bars, but without Octaform). It also increased the yield load by 65% and 91% for specimens D6 and D8 (150 mm and 200 mm depth respectively). The maximum load increased by about 36% on average for specimens D6 and D8.
 - b. Increased the deflection capacity (maximum deflection) of the Octaform-encased specimens by 24% and 55% for specimens D6 and D8 (150 mm and 200 mm depth respectively) compared to the control specimens.
- The behaviour of the Octaform-encased specimens was affected by the use of steel reinforcement in two different ways: 1) changed the saw-teeth behaviour in the load-deflection curve in the un-reinforced specimens to a continuous increase in the load as the deflection was increasing, and 2) The

presence of the steel reinforcement increased the load carrying capacity by 197% and the deflection by several folds.

- For the specimens reinforced with steel bars, the type of the connectors (flat in the middle or inclined in the corner) had no effect on the general behaviour of the Octaform-encased specimens
- For specimens without steel reinforcement, the yield and maximum load increased on average by 15% when both types of connectors were used as opposed to using one type. The increase was independent of the depth of the specimens. In addition, it was noted that the use of both types of connectors increased the rigidity of the specimens before concrete casting. However, the specimens with different connectors (inclined and middle) had similar behaviour.

Appendix A

Load-Deflection Behaviour

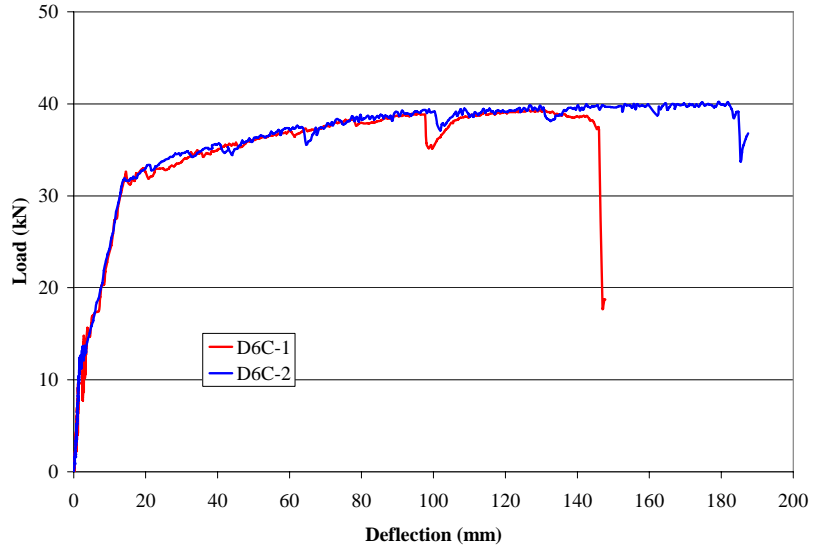


Figure A.1 Load-deflection curve for specimens D6C-1 and D6C-2

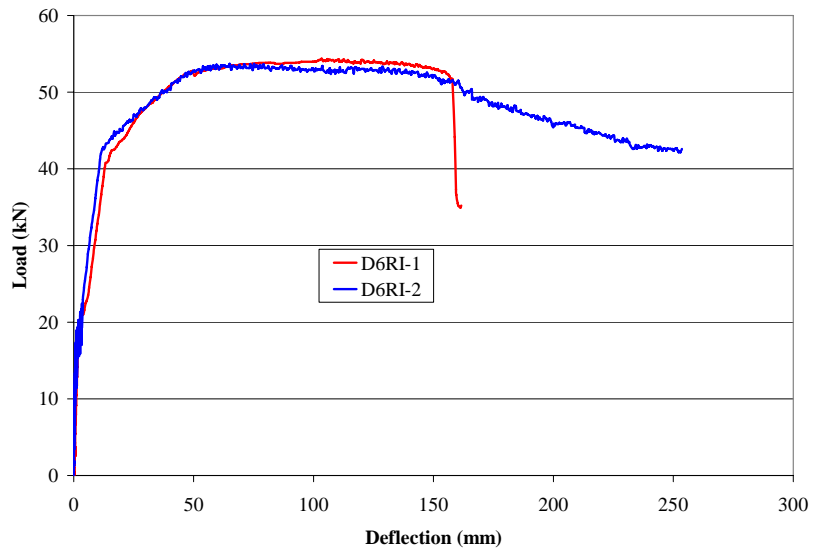


Figure A.2 Load-deflection curve for specimens D6RI-1 and D6RI-2

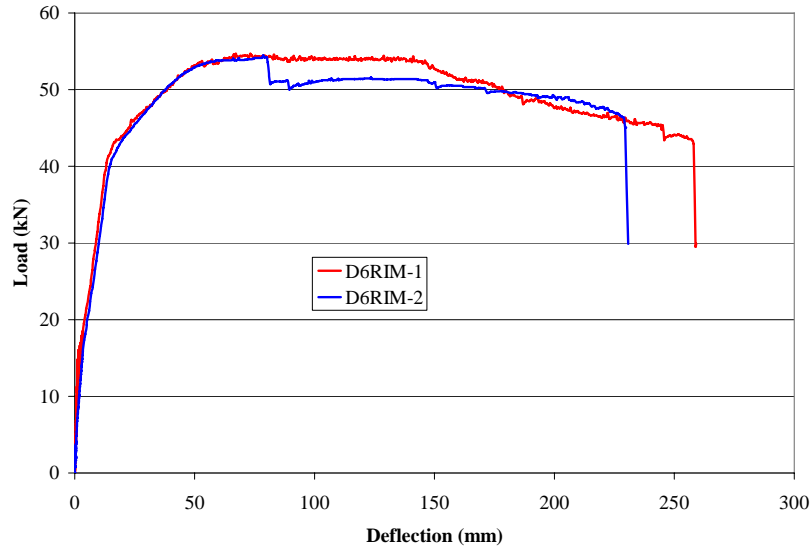


Figure A.3 Load-deflection curve for specimens D6RIM-1 and D6RIM-2

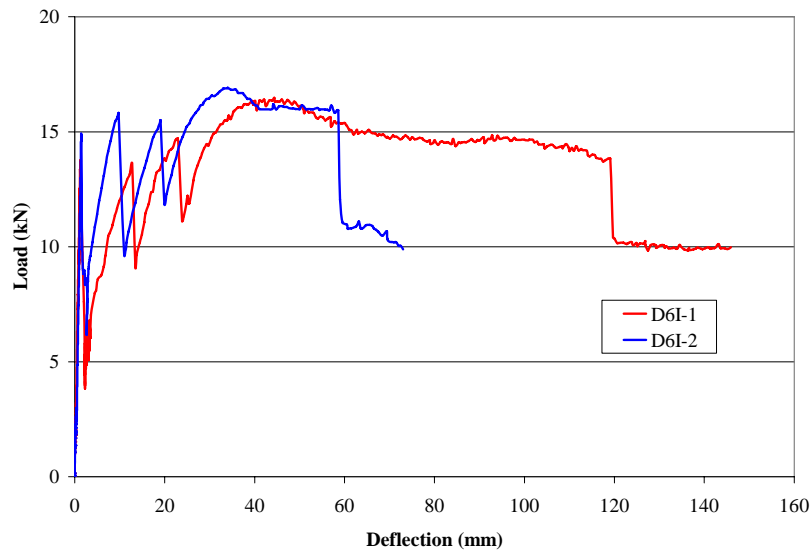


Figure A.4 Load-deflection curve for specimens D6I-1 and D6I-2

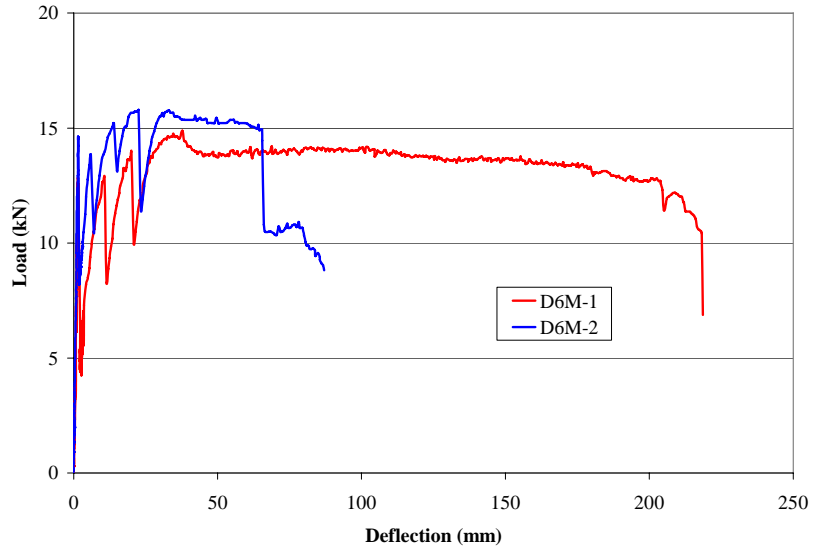


Figure A.5 Load-deflection curve for specimens D6M-1 and D6M-2

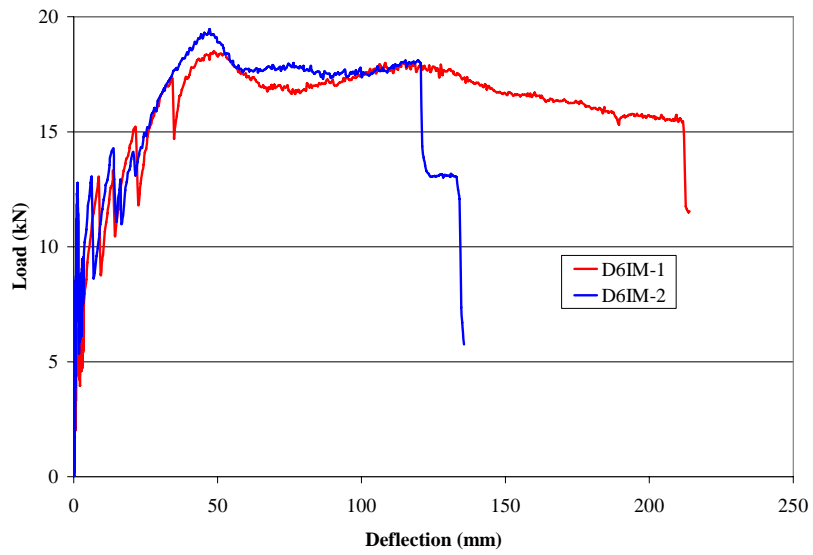


Figure A.6 Load-deflection curve for specimens D6IM-1 and D6IM-2

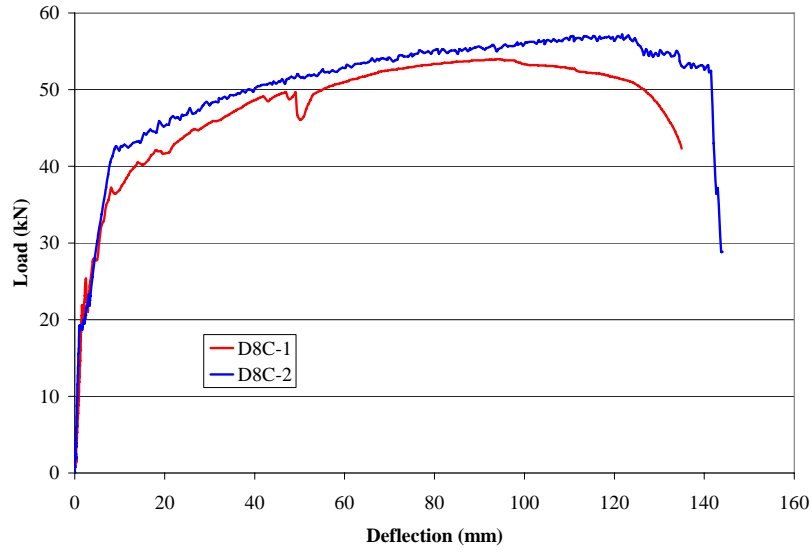


Figure A.7 Load-deflection curve for specimens D8C-1 and D8C-2

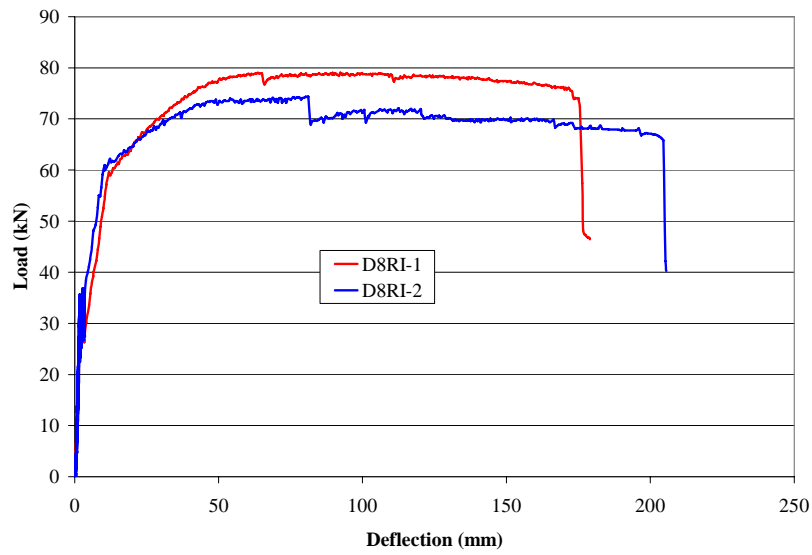


Figure A.8 Load-deflection curve for specimens D8RI-1 and D8RI-2

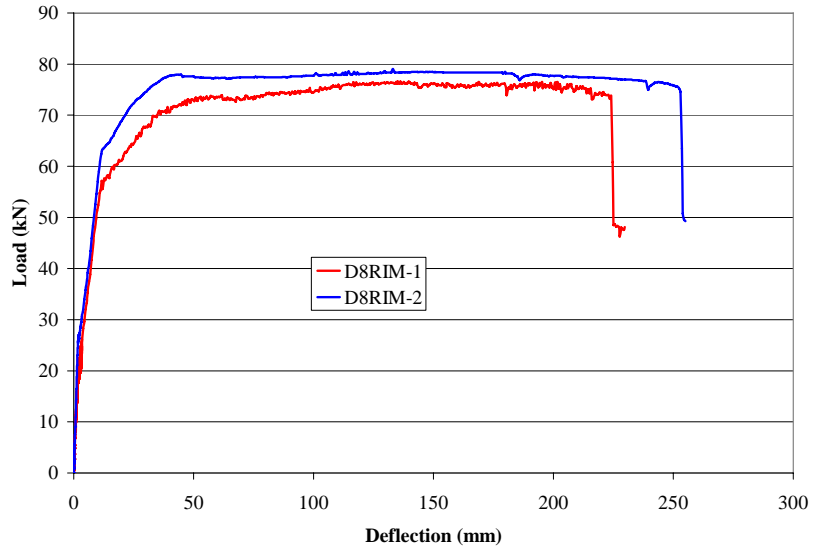


Figure A.9 Load-deflection curve for specimens D8RIM-1 and D8RIM-2

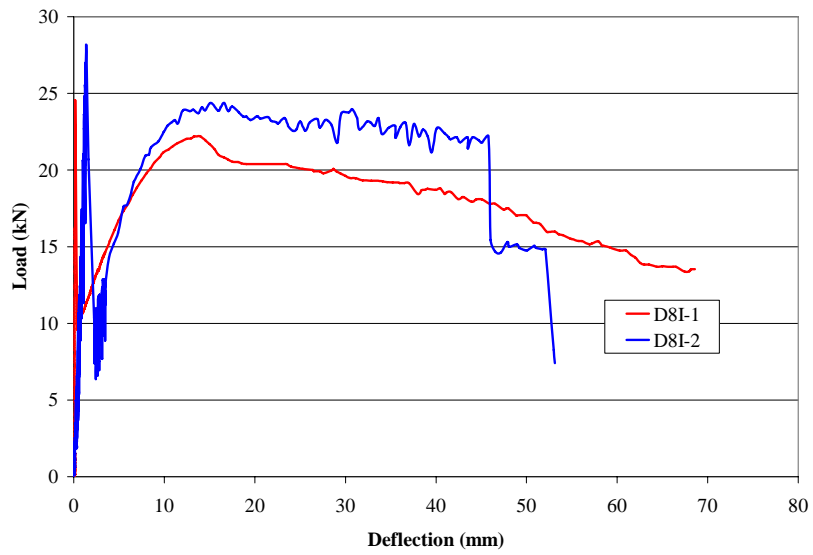


Figure A.10 Load-deflection curve for specimens D8I-1 and D8I-2

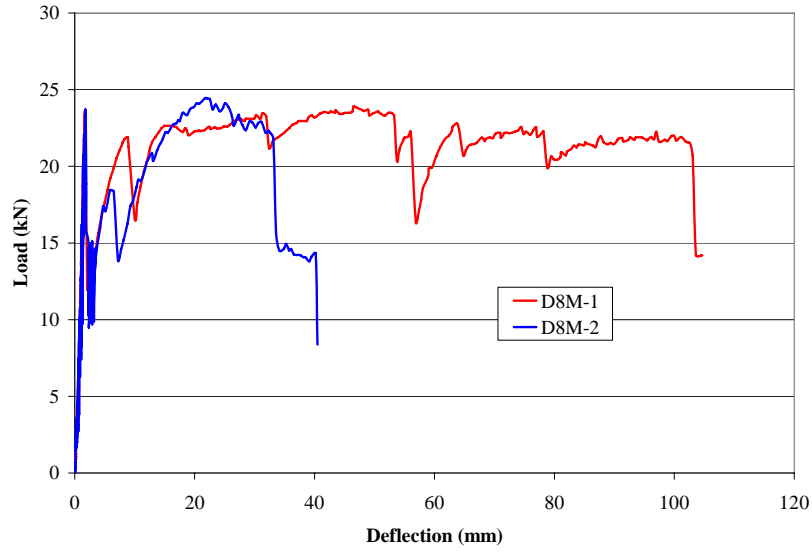


Figure A.11 Load-deflection curve for specimens D8M-1 and D8M-2

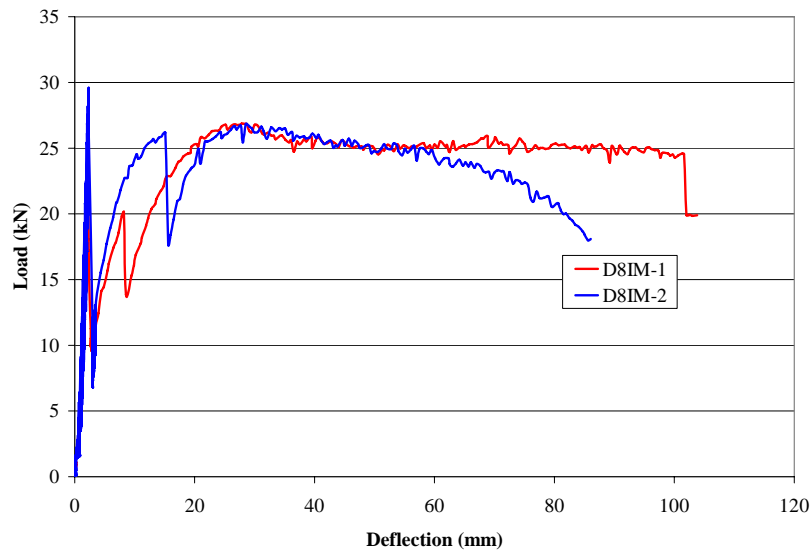


Figure A.12 Load-deflection curve for specimens D8IM-1 and D8IM-2

Acknowledgements

The authors would like to acknowledge the help of Mr. Chris Suffern and Mr. Ken Bowman during the various stages of lab work. In addition, the help of Mr. Terry Ridgway and Mr. Doug Hirst during casting is greatly appreciated.

References

- Octaform, 2004. "General Guide: version 2 revision 1." Octaform Systems, Vancouver, BC, 87 p.
- CSA 23.3, 2004. "Design of Concrete Structures." Canadian Standards Association, Toronto, ON.